Journal of Sound and Vibration 547 (2023) 117539

Contents lists available at ScienceDirect

Journal of Sound and Vibration

journal homepage: www.elsevier.com/locate/jsvi

Eddy currents damping understood as Zener viscoelastic damping

Fernando Cortés *, Ondiz Zarraga, Imanol Sarría, María Jesús Elejabarrieta

Department of Mechanics, Design and Industrial Management, University of Deusto, Avda. de las Universidades 24, 48007 Bilbao, Spain

ARTICLE INFO

Keywords:
Eddy currents
Zener viscoelastic model
Relaxation time
Self-inductance

ABSTRACT

This paper identifies and explains the eddy currents damping originated in a solid that vibrates in a magnetic field as a Zener viscoelastic model damping. For that, a coupled mechanical-electrical model is proposed for the eddy currents damping. The mechanical model is studied as a single degree-of-freedom system, and the electrical model is assumed to be a closed *RL* circuit. The coupling between them is given by the magnetic force originated by the motional inductance. The motion equation is obtained for the coupled system for two different excitation types: harmonic force and harmonic base motion. These motion equations include derivatives of the displacement with respect to time up to the third order. An equivalence between these motion equations and the ones derived for a viscoelastic system modelled with a Zener model is found. This allows understanding the parameters of the eddy currents model as the ones of a viscoelastic Zener model. The term related with the third order derivative is associated with relaxation, a characteristic property of viscoelastic systems. This equivalence between Zener and eddy currents damping explains forces proportional to the third order derivative that other authors have experimentally found in vibrating systems with eddy currents. The proposed model is validated both from an analytical comparison with another model of the literature and from experimental results previously published. Finally, a parametric study is carried out to show up the influence of the magnetic field and electrical properties of the model on the frequency and time responses of the system.

1. Introduction

When a non-magnetic and metallic conductor moves in an external magnetic field, Foucault currents appear, also known as eddy currents. These eddy currents, which have been studied since the nineteenth century, can be a problem for the correct working of many systems, going from transformers [1] to vacuum chambers in synchrotrons [2]. But, at the same time, eddy currents can be very useful in many different applications. For example, they provide non-destructive probing tests to find cracks in metal plates [3], and levitation melting uses eddy currents to avoid the contamination of containers with certain particles [4,5]. Also, many authors have proposed the use of eddy currents to act on dynamical systems, such as magnetic breaks [6,7], dampers for seismic excitations [8], and lever-type vibration isolators [9]. Some studies such as [10] and [11] presented a thorough review of these varied applications.

Non-contact passive electromagnetic dampers have been used since a long time ago. The main advantage of using the phenomenon of eddy currents to attenuate structural vibration is the possibility of removing energy from the system without contact with the structure itself [10]. Studies focusing on this non-contact feature have shown that the natural frequencies of the structure are not

* Corresponding author.
E-mail addresses: fernando.cortes@deusto.es (F. Cortés), ondiz.zarraga@deusto.es (O. Zarraga), isarria@deusto.es (I. Sarría), maria.elejabarrieta@deusto.es (M.J. Elejabarrieta).

https://doi.org/10.1016/j.jsv.2022.117539
Received 9 September 2022; Received in revised form 25 November 2022; Accepted 22 December 2022
Available online 23 December 2022

changed in such cases [12,13]. In addition, unlike other damping techniques, such as viscoelastic materials or piezoelectric actuators, no mass is added to the structure to be damped. Most of the works that analyse the eddy currents phenomenon have focused on designing eddy currents devices that significantly magnify the damping added to the structure, but resulting also in a significant modification of the original structural properties [10–13].

The modelling and analysis of eddy currents and their induced damping have been tackled from several angles in the last decades, given the great importance of these electromagnetic-mechanical coupling for many engineering devices [14,15]. For all its practical applications, the mathematical theory and models behind eddy currents induction are notoriously complex. There is a lack of simple models and methods capable of describing the influence of eddy currents induced by different magnetic field configurations. Recently Loong et al. [16] have modelled the forces involved in the damping from the eddy currents as a Kelvin-Voigt model in a magneto-quasistatic approximation, and these forces have also been studied with a fractional Kelvin-Voigt model in parallel acting on an equivalent *RL* circuit [17], for instance. In any case, it has been shown that both the self-inductance and the jerk (the derivative of the acceleration) are crucial in order to fit any of these results to experimental data.

From this background, this work presents the eddy currents damping effect understood as a Zener viscoelastic model, therefore showing an equivalence between the mechanical and the electromagnetic areas of research. This viscoelastic model is simple and well known in the field of rheology, which helps to interpret the effects of the currents in the system as well as to identify the self-inductance as a mechanical relaxation of the system. In the mechanical-electrical model proposed in this paper, it can be found that the third order derivative of the displacement obtained is equivalent to that found in a Zener viscoelastic model. This third order derivative describes the relaxation of the system. Considering that the relaxation from the electrical part is associated to the self-inductance, and applying these ideas to a system subjected to eddy currents, it is shown a perfect match between the damping coming from eddy currents and that which is characteristic to a Zener viscoelastic model. Besides these advantages associated to the model, it also explains the experimental results obtained by [16,18] and agrees with previous analytical results [17]. Also, the present work could make the engineering problem of the design of eddy currents dampers easier, due to the correlation of these systems with the well-known Zener viscoelastic model.

In short, in this paper, a theoretical background on Zener viscoelastic model is presented. Next, a coupled mechanical-electrical model for the eddy currents is proposed for two different types of excitations, namely, harmonic force and harmonic base motion, and the equivalence with the Zener viscoelastic model is analysed. Then, a validation of the model is presented, both with an analytical comparison with another model of other authors [17], and with experimental results previously published [18]. Finally, a parametric study is performed to reveal the influence of some parameters on the response of the system. On the one hand, the influence of the magnetic field strength on the frequency transmissibility function is studied. And on the other hand, it has been analysed the influence of the electrical properties on the time response, relating them with the damping factors of the equivalent Zener model.

2. Brief background on Zener viscoelastic model

The Zener model, also known as the Standard Linear Solid (SLS) model, is a method to model the behaviour of viscoelastic materials by means of a linear combination of two springs and a dashpot. This is the simplest model able to reproduce creep and relaxation, both phenomena being characteristics of the viscoelastic behaviour. Therefore, this model is said to have memory, i.e., the current response is a result of the complete history of the system.

In this Section, the governing equations of a vibrating single degree-of-freedom (DOF) system with Zener damping are presented for two different excitation types. The first case is a system excited by a force, and the second one is a system subjected to a base motion. These two cases are employed for the analogy with eddy currents damping in Section 3 and in the validation of Section 4.

2.1. Case 1: forced response

Fig. 1 represents a forced single degree-of-freedom system in which the viscoelasticity has been modelled by means of a Zener model. The external force is $f(t)$, the mass of the system is m, the stiffness of the in-parallel spring is k_0, and the stiffness and viscous

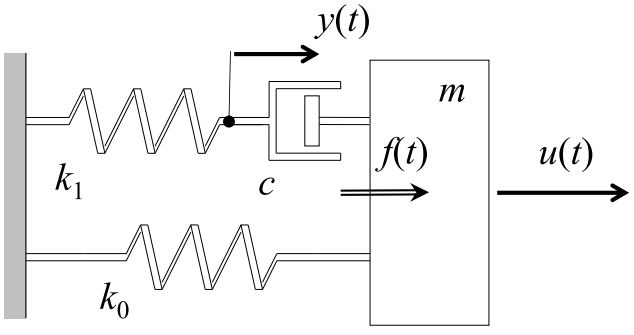

Fig. 1. Representation of the Zener model in a forced single degree-of-freedom system.

coefficient of the in-series spring and dashpot are k_1 and c, respectively. The motion equation for the displacement $u(t)$ is given by

$$m\,\ddot{u}(t) + c(\dot{u}(t) - \dot{y}(t)) + k_0\,u(t) = f(t), \tag{1}$$

where $y(t)$ is an internal variable that represents the displacement of the connecting point between the in-series spring and the dashpot. The force equilibrium in this point implies that

$$k_1\,y(t) = c(\dot{u}(t) - \dot{y}(t)). \tag{2}$$

This set of two differential equations with two unknowns, $u(t)$ and $y(t)$, can be solved by different ways. García-Barruetabeña et al. [19] discussed on two different methods, one solving the internal variable $y(t)$ and the other one without solving the internal variable. The latter consists in the transformation of Eq. (1) and (2) in linear algebraic equations by operational calculus, yielding

$$\left[\frac{c}{k_1}m\,s^3 + m\,s^2 + \frac{c}{k_1}(k_0+k_1)s + k_0\right]U(s) = \left(\frac{c}{k_1}s + 1\right)F(s), \tag{3}$$

where $U(s)$ and $F(s)$ are the Laplace transforms of $u(t)$ and of $f(t)$, respectively. By means of the inverse transform, the corresponding third order differential equation results in

$$\tau\,m\,\dddot{u}(t) + m\,\ddot{u}(t) + \tau(k_0+k_1)\dot{u}(t) + k_0u(t) = \tau\dot{f}(t) + f(t), \tag{4}$$

where τ is defined as the relaxation time of the system, which is given by

$$\tau = \frac{c}{k_1}. \tag{5}$$

A force proportional to the derivative of the acceleration $\dddot{u}(t)$ (known as jerk) appears in Eq. (4). This force is what provides relaxation into the system, i.e., it is zero when the relaxation time τ is zero, and in that case the system behaves as a viscous one, without relaxation.

2.2. Case 2: base motion

In this second case, the single degree-of-freedom system of the previous case is subjected to a base displacement $z(t)$ instead to a force, as represented in Fig. 2.

Here the motion equation is given by

$$m\,\ddot{u}(t) + c(\dot{u}(t) - \dot{y}(t)) + k_0\,(u(t) - z(t)) = 0, \tag{6}$$

and the equation of the force equilibrium at the connection point of the model is

$$k_1\,(y(t) - z(t)) = c(\dot{u}(t) - \dot{y}(t)). \tag{7}$$

Making use of the operational calculus in an equivalent way to that in Case 1, the resulting equation yields

$$\tau\,m\,\dddot{u}(t) + m\,\ddot{u}(t) + \tau(k_0+k_1)\dot{u}(t) + k_0u(t) = \tau(k_0+k_1)\dot{z}(t) + k_0z(t), \tag{8}$$

where the right-hand term of the equation represents the force that must be applied to the base to obtain the desired movement.

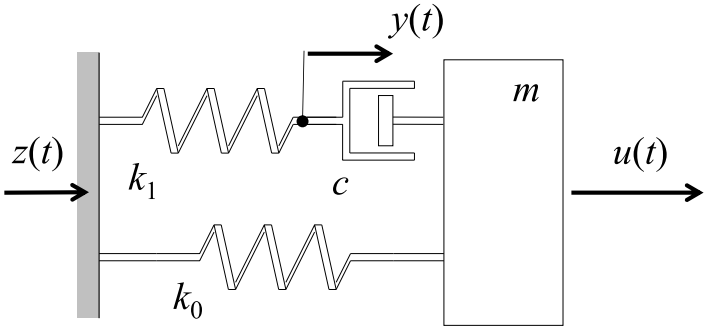

Fig. 2. Representation of the Zener model in a single degree-of-freedom system with base motion.

3. Eddy currents damping model and analogy with Zener

Let us consider a metallic solid that vibrates in a uniform magnetic field. Eddy currents appear in this solid due to the motional inductance, which implies Joule's losses that dissipate mechanical energy to heat. From the mechanical point of view, this energy dissipation is due to the magnetic force that appears by the interaction between the induced eddy currents and the imposed magnetic field. Therefore, the vibration is attenuated by the eddy currents, and these effects can be named as eddy currents damping.

In order to present an analogy between the eddy currents damping and a Zener viscoelastic damping, in this section the motion of a metallic bar vibrating in a uniform time-invariant magnetic field is modelled as a single degree-of-freedom system. Two different cases are studied: first the case of the bar subjected to an external force $f(t)$, and next the case of the base motion.

3.1. Case 1: forced response

Fig. 3 represents the bar attached to a set of springs of global stiffness k_0. The mass of the bar is m and its length is ℓ. The bar slides without friction over metallic rails, conforming a closed electrical line, whose contour is C. The bar moves in the x direction, the displacement being $\mathbf{u}(t) = u(t)\,\mathbf{x}$. The governing equation of the motion of the bar is given by

$$m\,\ddot{u}(t) + k_0\,u(t) = f_{\mathrm{m}}(t) + f(t), \tag{9}$$

where the external forces are separated into the contribution of the magnetic force $f_{\mathrm{m}}(t)$ and that of the rest of the external forces $f(t)$. The magnetic force experienced by the metallic bar is determined next.

The magnetic field is uniform and constant in the z direction, represented by the magnetic intensity $\mathbf{B} = B\,\mathbf{z}$. An electromotive force $\mathscr{E}_{\mathrm{ind}}$ is induced by motional inductance, known as motional EMF (see any textbook on the field, for instance [20]), given by

$$\mathscr{E}_{\mathrm{ind}} = \oint_C (\dot{\mathbf{u}} \times \mathbf{B}) \cdot \mathrm{d}\mathbf{l}, \tag{10}$$

where the integral along the closed contour C results in

$$\mathscr{E}_{\mathrm{ind}}(t) = \dot{u}(t)\,B\,\ell. \tag{11}$$

This motional EMF induces a current $i(t)$ in the line, in which the resistance R and the inductance L are actually the resistance and the self-inductance of the metallic solid in which the eddy currents appear. The equation that governs the circuit is

$$L\frac{\mathrm{d}i(t)}{\mathrm{d}t} + R\,i(t) = \mathscr{E}_{\mathrm{ind}}(i), \tag{12}$$

wherefrom the magnetoelectrical and mechanical coupling results in

$$L\frac{\mathrm{d}i(t)}{\mathrm{d}t} + R\,i(t) = \dot{u}(t)\,B\,\ell. \tag{13}$$

The magnetoelectrical-mechanical coupling is also given by the magnetic force $f_{\mathrm{m}}(t)$ acting of the bar, that according to Lorentz law, is given by

$$\mathbf{f}_{\mathrm{m}}(t) = i(t)\mathbf{l} \times \mathbf{B}, \tag{14}$$

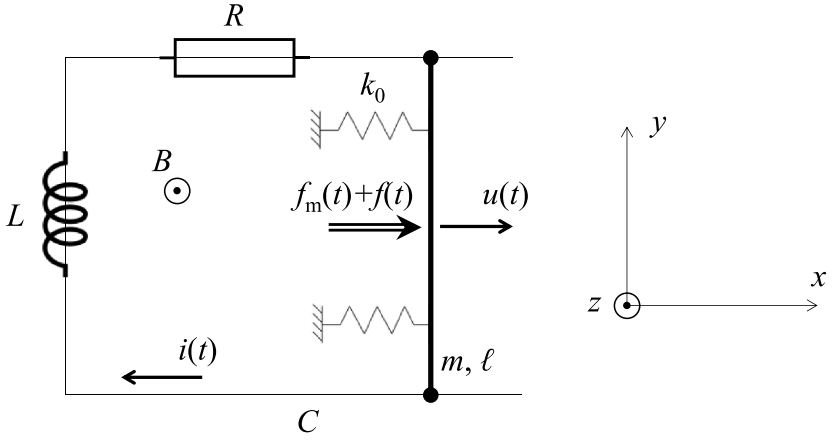

Fig. 3. Representation of a forced single degree-of-freedom system moving in a uniform and time-invariant magnetic field, in which an induced current in an equivalent RL circuit appears.

where $\mathbf{l} = -\ell\,\mathbf{y}$. Thus, the magnetic force yields

$$f_{\mathrm{m}}(t) = -i(t)B\ell, \tag{15}$$

where the negative sign implies that the sense of this force is the opposite to that represented in Fig. 3.

Summarizing, a set of three differential equations is reached, given by Eqs. (9), (13) and (15), the three unknowns being the displacement $u(t)$, the current intensity $i(t)$and the magnetic force $f_{\mathrm{m}}(t)$. This may be transformed into an algebraic linear system by means of operational calculus, resulting in

$$\left(s^2 m + k_0\right) U(s) = F_{\mathrm{m}}(s) + F(s), \tag{16}$$

$$(sL + R) I(s) = sU(s) B\,\ell \tag{17}$$

and

$$F_{\mathrm{m}}(s) = -I(s)B\ell, \tag{18}$$

where $U(s)$, $I(s)$, $F_{\mathrm{m}}(s)$ and $F(s)$ are the Laplace transform of $u(t)$, $i(t)$, $f_{\mathrm{m}}(t)$ and $f(t)$. As a result, the next equation is obtained for the displacement,

$$\left[\frac{L}{R} m s^3 + m s^2 + \frac{L}{R}\left(k_0 + \frac{B^2\ell^2}{L}\right) s + k_0\right] U(s) = \left(\frac{L}{R} s + 1\right) F(s), \tag{19}$$

whose differential equation yields

$$\frac{L}{R} m \dddot{u}(t) + m\,\ddot{u}(t) + \frac{L}{R}\left(k_0 + \frac{B^2\ell^2}{L}\right)\dot{u}(t) + k_0 u(t) = \frac{L}{R}\dot{f}(t) + f(t). \tag{20}$$

On one hand, it can be pointed out that this differential equation is the same as that of the Zener model given by the Eq. (4). In this context, the equivalent stiffness k_1 is given by

$$k_1 = \frac{B^2\ell^2}{L}, \tag{21}$$

the equivalent viscous coefficient c of the dashpot is given by

$$c = \frac{B^2\ell^2}{R}, \tag{22}$$

and, consequently, the equivalent relaxation time τ is

$$\tau = \frac{L}{R}, \tag{23}$$

which beautifully coincides with the time constant of a *RL* circuit. It also should be noted that, if the self-inductance of the bar is negligible, the Zener model derives in the Kelvin-Voigt model, resulting

$$m\,\ddot{u}(t) + \frac{B^2\ell^2}{R}\dot{u}(t) + k_0 u(t) = f(t), \tag{24}$$

that is, the dissipative forces derived by the eddy currents would be purely viscous. Hence, the self-inductance is the property allowing the relaxation of the system, a characteristic of viscoelastic systems described by a Zener model, as opposed to the viscous behaviour described by a Kelvin-Voigt model. Indeed, as Eq. (23) shows, a zero self-inductance implies no relaxation.

On the other hand, according to Eq. (20), it can be noted that the eddy currents damping involves forces proportional to the first and third derivatives of the displacement with respect to time. Hence, this model justifies two of the three kinds of forces that [16] proposed to be fitted to experimental results. However, Eq. (20) does not explain forces related to the acceleration. This is because eddy currents do not imply inertial forces since they have a dissipative nature.

Finally, as for the internal variable $y(t)$ of the Zener model described in Section 2, this eddy currents model yields

$$\frac{B^2\ell^2}{L} y(t) = \frac{B^2\ell^2}{R}\left(\dot{u}(t) - \dot{y}(t)\right), \tag{25}$$

that is,

$$L\,\dot{y}(t) + R\,y(t) = L\,\dot{u}(t). \tag{26}$$

This last equation is the same as Eq. (13) if the internal variable $y(t)$ is defined as

$$y(t) = \frac{L}{B}\frac{i(t)}{\ell}. \tag{27}$$

Thus, in the Zener model equivalent to eddy currents damping, the internal variable is proportionally related to the current intensity linear density $i(t)/\ell$. If the last equation is written as

$$L\, i(t) = B\ell\, y(t), \tag{28}$$

the left-hand side represents the magnetic flux generated by the induced current, and the right-hand side represents the flux of the impressed magnetic field of intensity B, over an area $\ell\, y(t)$.

3.2. Case 2: base motion

In this second case, represented in Fig. 4, the electric circuit and the base at which the springs set is attached has a motion characterised by $z(t)$.

The governing equation of the motion of the bar is given by

$$m\,\ddot{u}(t) + k_0\,(u(t) - z(t)) = f_{\mathrm{m}}(t), \tag{29}$$

where the magnetic force $f_{\mathrm{m}}(t)$ is given again by Eq. (15), but in this case, the induced current is not given by (13), because the circuit has also the movement of the base. Instead, it is given by

$$L\frac{\mathrm{d}i(t)}{\mathrm{d}t} + R\, i(t) = (\dot{u}(t) - \dot{z}(t))\, B\, \ell. \tag{30}$$

Then, making use of the operational calculus as in the previous case, the resulting differential equation yields

$$\frac{L}{R}m\dddot{u}(t) + m\,\ddot{u}(t) + \frac{L}{R}\left(k_0 + \frac{B^2\ell^2}{L}\right)\dot{u}(t) + k_0 u(t) = \frac{L}{R}\left(k_0 + \frac{B^2\ell^2}{L}\right)\dot{z}(t) + k_0 z(t), \tag{31}$$

which is equivalent to Eq. (8) of the mechanical model of Section 2.3, using again the assumptions of Eqs. (21)-(23).

4. Validation

The validation is carried out from two points of view, one analytical and the other experimental. Firstly, the eddy currents force of Case 1 of the previous sections is compared with the analytical results of the non-linear model published in [17]. Next, from the response of the base motion of Case 2, a transmissibility function is obtained and compared with experimental transmissibility measures carried out on an aluminium cantilever beam that vibrates in a magnetic field, previously published by one of the authors in [18].

4.1. Comparison with an analytical forced response

Shi et al. [17] presented a non-linear model for the eddy currents damping forces based on a viscous damping model in which damping force $f_{\mathrm{EC,NLV}}(t)$ is non-linearly proportional to velocity $\dot{u}(t)$,

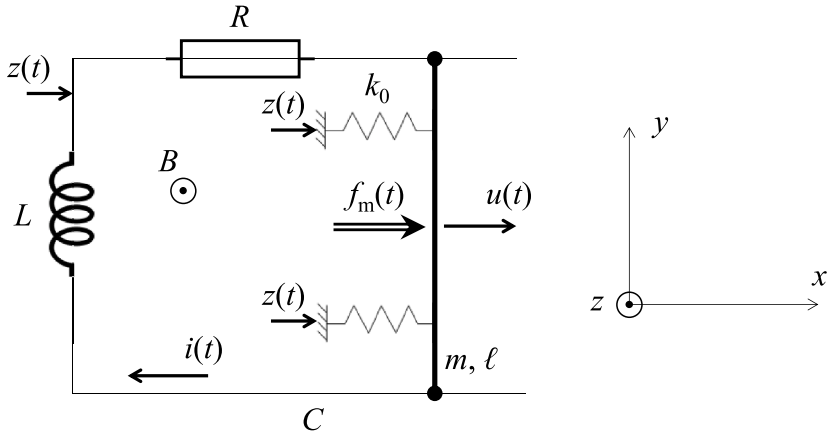

Fig. 4. Representation of a single degree-of-freedom system moving in a uniform and time-invariant magnetic field, in which an induced current in an equivalent *RL* circuit appears, and the base moves.

$$f_{\mathrm{EC,NLV}}(t) = C(t)\,\dot{u}(t), \tag{32}$$

i.e., the parameter $C(t)$ varies with time. For the particular case of a harmonic velocity given by

$$\dot{u}(t) = V_{\mathrm{m}}\cos\omega t, \tag{33}$$

where V_{m} is the amplitude and ω is the angular frequency, the eddy currents force results in [17].

$$f_{\mathrm{EC,NLV}}(t) = c_1 \mathrm{e}^{-\frac{t}{\tau}} + \frac{cV_{\mathrm{m}}\cos(\omega t+\theta)}{\sqrt{1+\omega^2\tau^2}}, \tag{34}$$

where c_1 is a constant with units of force, c is the equivalent viscous coefficient given by Eq. (22), τ is the relaxation time given by Eq. (23), and the phase angle θ satisfies

$$\tan\theta = -\omega\tau. \tag{35}$$

Next, let us get the eddy currents damping force $f_{\mathrm{EC,Z}}(t)$ according to the model presented in this paper based on the linear Zener model. This force is given by the magnetic force of Eq. (15) but with a plus sign, and making use Eqs. (17) and (18), the Laplace transform of this force gives

$$F_{\mathrm{EC,Z}}(s) = \frac{\dot{U}(s)B^2\ell^2}{Ls+R}, \tag{36}$$

that, by means of Eqs. (22) and (23), it may be transformed into

$$F_{\mathrm{EC,Z}}(s) = c\frac{\dot{U}(s)}{s\tau+1}. \tag{37}$$

Taking into account Eq. (33), *i.e.* that the velocity is harmonic, the Laplace transform of the force results in

$$F_{\mathrm{EC,Z}}(s) = cV_{\mathrm{m}}\frac{s}{(s^2+\omega^2)(s\tau+1)}. \tag{38}$$

To apply the inverse Laplace transform, this equation must be decomposed in partial fractions as

$$F_{\mathrm{EC,Z}}(s) = cV_{\mathrm{m}}\left(\frac{-1}{1+\omega^2\tau^2}\cdot\frac{\tau}{s\tau+1} + \frac{1}{\sqrt{1+\omega^2\tau^2}}\cdot\frac{s\frac{1}{\sqrt{1+\omega^2\tau^2}} - \omega\frac{-\omega\tau}{\sqrt{1+\omega^2\tau^2}}}{s^2+\omega^2}\right). \tag{39}$$

The inverse Laplace transform this equation yields

$$f_{\mathrm{EC,Z}}(t) = \frac{-cV_{\mathrm{m}}}{1+\omega^2\tau^2}\mathrm{e}^{-\frac{t}{\tau}} + \frac{cV_{\mathrm{m}}}{\sqrt{1+\omega^2\tau^2}}\cos(\omega t+\theta). \tag{40}$$

This equation for the eddy currents damping force obtained with the proposed model is equivalent to the one of Shi et al. [17] given by Eq. (34), because Eq. (35) is satisfied and the constant c_1 shoud be

$$c_1 = \frac{-cV_{\mathrm{m}}}{1+\omega^2\tau^2}, \tag{41}$$

that actually depends on the angular frequency ω.

4.2. Comparison with experimental transmissibility measurements

In this Section the model is validated by the comparison with experimental results. Specifically, the parameters of the transmissibility function obtained from Case 2 of the previous sections are obtained by curve fitting, using transmissibility experimental data. For that, let us considerer a harmonic base motion given by

$$z(t) = Z_0\mathrm{e}^{\mathrm{i}\omega t}, \tag{42}$$

where Z_0 is the amplitude and ω is the angular frequency of the motion. Then, the displacement $u(t)$ is also harmonic with the same angular frecency and complex amplitude U_0 that can be solved from Eq. (8), transformed in

$$\left[-\mathrm{i}\omega^3\tau\,m - \omega^2\,m + \mathrm{i}\omega\tau(k_0+k_1)+k_0\right]U_0 = \left[\mathrm{i}\omega\tau(k_0+k_1)+k_0\right]Z_0. \tag{43}$$

From this equation, the complex transmisibility function $T(\omega)$, defined as the ratio between U_0 and Z_0, gives

$$T(\omega) = \frac{\mathrm{i}\omega\tau(k_0+k_1)+k_0}{-\mathrm{i}\omega^3\tau\,m - \omega^2\,m + \mathrm{i}\omega\tau(k_0+k_1)+k_0}, \tag{44}$$

which can be transformed with non-dimensional parameters as

$$T(r) = \frac{\mathrm{i}(\beta + 2\zeta)r + 1}{-\mathrm{i}\beta r^3 - r^2 + \mathrm{i}(\beta + 2\zeta)r + 1}, \tag{45}$$

where $r = \omega/\omega_\mathrm{n}$ is the normalised frequency, and ω_n, ζ and β are the natural frequency of the undamped system, the well-known viscous damping factor, and the non-viscous damping factor [21], given by

$$\omega_\mathrm{n} = \sqrt{k_0/m}, \tag{46}$$

$$\zeta = c/2\,m\,\omega_\mathrm{n} \tag{47}$$

and

$$\beta = \tau\,\omega_\mathrm{n}, \tag{48}$$

respectively. In the particular case in which the effect of the non-viscous damping factor β parameter is negligible with respect to the effect of the other terms, Eq. (45) becomes

$$T(r) = \frac{\mathrm{i}2\zeta r + 1}{-r^2 + \mathrm{i}2\zeta r + 1}, \tag{49}$$

which corresponds to the transmissibility derived from the Kelvin-Voigt model. Therefore, it can be remarked that for the transmissibility function, the gain of the Zener model is more important as the parameter β is more significant, *i.e.* as the self-inductance plays a bigger role.

For the validation, next Eq. (45) is fitted to transmissibility experimental data and the parameters of the system are identified. The experimental data for the validation where published previously in [18]. Specifically, let us model the vibration due to the second mode of a cantilever beam made of aluminium as a single DOF system. The second mode has been chosen as an example in this validation because its measurement quality. The geometrical properties of the beam are: vibrating length $\ell = 180$ mm, width $a = 9.93$ mm, and thickness $h = 0.404$ mm. The material properties are: electrical conductivity $\sigma = 3.77 \times 10^7$ S/m, and density $\rho = 2770$ kg/m^3. Thus, the mass of the beam is$m_\mathrm{beam} = 2.00 \times 10^{-3}$kg. The mean value of the applied magnetic field intensity is $B_0 = 68.8 \times 10^{-3}$ T (see [18] for more details about the experimental measurements).

For the equivalent single degree-of-freedom system, the equivalent vibrating mass of the second mode of a cantilever beam is $m = 0.25\,m_\mathrm{beam}$ [22]. The natural frequency obtained in [18] is $f_\mathrm{n} = 61.9$ Hz, or $\omega_\mathrm{n} = 388.9$ rad/s. The rest of the parameters are obtained by the curve fitting of Eq. (45) by means of the minimization of the objective function

$$g(\mathbf{x}) = \sum_{k=k_\mathrm{min}}^{k_\mathrm{max}} |T_k - T(r_k)|, \tag{50}$$

where k_min and k_max denote the indexes of the minimum and maximum frequencies to adequately represent the second mode, T_k is the value of the complex experimental transmissibility at the normalised angular frequency r_k, and $\mathbf{x}$ is the unknown array conformed by the parameters β and ζ. These results derived of the curve fitting and the corresponding parameters of the Zener and the mechanical-electrical models are summarized in Table 1.

The result of the curve fitting procedure is shown in Fig. 5, in which the Eq. (45) is compared with the experimental transmissibility curve [18].

It can be concluded that the fitted curve matches the experimental results both in modulus and phase. The small differences may be due to the fact that the magnetic field is not uniform throughout the beam. From an analysis of the theoretical curve, it can be pointed out that, in this case, the resonance frequency is almost the same as the undamped natural frequency, *i.e.*, 61.9 Hz, as was exhaustively studied in [18].

5. Parametric study

This Section presents a parametric study aimed at illustrating the influence of some properties of the model on the frequency and time responses. Specifically, on the one hand the influence of the magnitude of the magnetic field intensity on the frequency transmissibility is studied. And on the other hand, an analysis is performed to reveal the influence on the time response of the electrical

Table 1
Properties of the mechanical and mechanical-electrical models.

Common properties Experimental data		Curve fitting		Eqs. (46) & (48)		Mechanical model Eqs. (47) & (5)		Electrical model Eqs. (21) & (22)	
m (g)	ω_n (rad/s)	β (−)	ζ (−)	k_0 (N/m)	τ (ms)	c (Ns/m)	k_1 (N/m)	L (μH)	R (mΩ)
0.50	388.9	0.051	0.0055	75.6	0.013	0.021	16.3	7.83	59.7

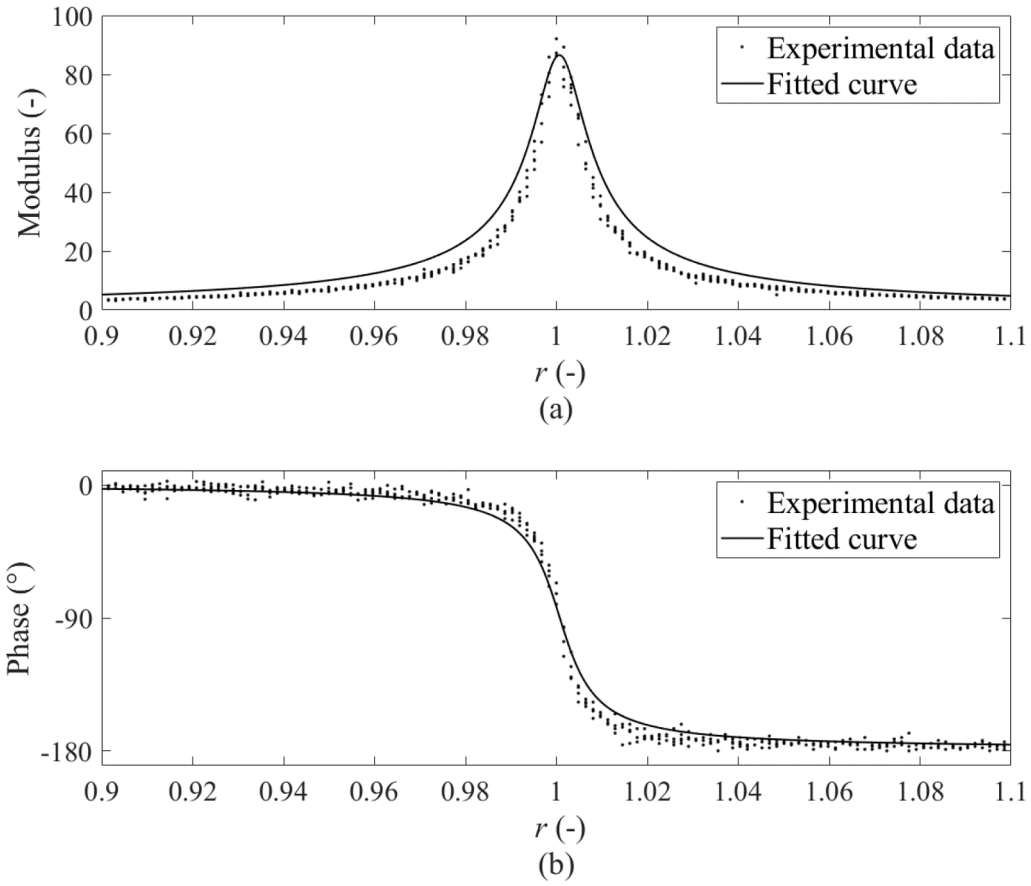

Fig. 5. Transmissibility experimental data and fitted curve base on Zener model: (a) modulus and (b) phase.

properties L and R of the system, which are related with the damping factors β and ζ.

5.1. *Effect of the magnetic field intensity on frequency transmissibility*

The transmissibility of the single-degree of freedom system given by Eq. (45) of Section 4 is computed for three increasing different values of the magnetic field intensity B. The three studied cases are the following:

- Case 1: The magnetic field intensity is the reference value of the validation of Section 4.2, *i.e.* $B_1 = B_0 = 68.8 \times 10^{-3}$ T.
- Case 2: The magnetic field intensity is 1.5 times bigger than the reference value, $B_2 = 1.5B_0 = 103.2 \times 10^{-3}$ T.
- Case 3: The magnetic field intensity is 2 times bigger than the reference value, $B_3 = 2B_0 = 137.6 \times 10^{-3}$ T.

The curves obtained of the modulus and phase of the transmissibility as a function of the normalised frequency r are presented in Fig. 6 for the frequency range comprised between the 90% and the 110% of the natural frequency f_n.

This figure shows that the magnetic field intensity B is directly related with the vibration attenuation of the system: the bigger B, the higher the attenuation. In fact, B is related with the damping viscous coefficient c, as it was shown in Eq. (22). Specifically, by increasing the magnetic field intensity B by 1.5 and 2 times, the amplitude of the transmissibility resonance peak is reduced from 91.1 to 40.5 and to 22.8, respectively, *i.e.*, the amplitude is reduced by 55.5% and in 74.9%. These results show that in engineering applications, the damping capacity of a system may be controlled by the magnetic field intensity B.

5.2. *Influence of the electrical properties on time response*

In this Section the influence that the viscous damping factor ζ and the non-viscous damping factor β have on the time response of the system is studied. For that, the free vibration of a system that starts at rest and is subjected to an initial displacement u_0 is considered. In free vibration, Eq. (20) becomes

$$\beta \dddot{u}(t) + \omega_n \ddot{u}(t) + \omega_n^2(\beta + 2\zeta)\dot{u}(t) + \omega_n^3 u(t) = 0. \tag{51}$$

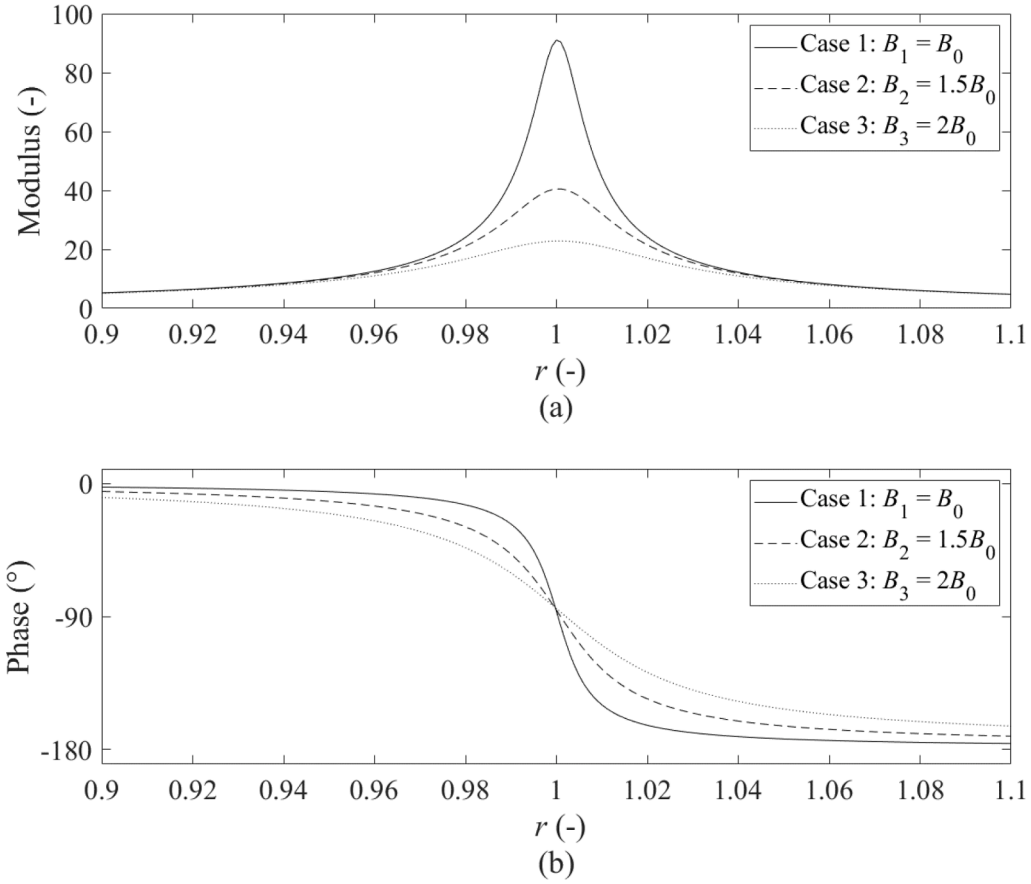

Fig. 6. Transmissibility functions for three increasing magnetic field intensities: (a) modulus and (b) phase.

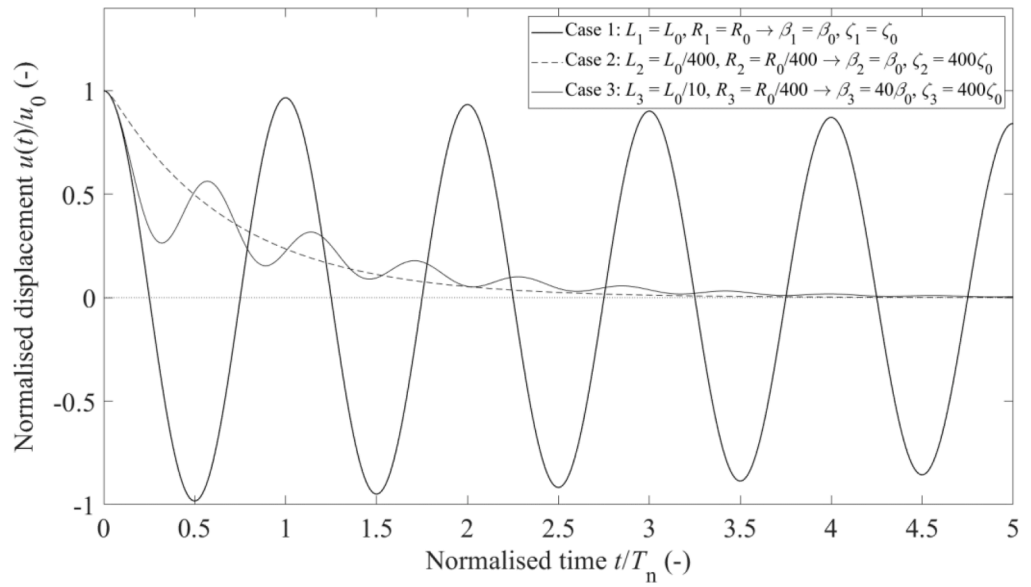

Fig. 7. Time response of the system for three different pairs of L and R, corresponding to three different pairs of damping factors β and ζ.

This equation may be solved by means of the Runge-Kutta method with the following initial conditions: $u_0 = 10^{-3}$m, $\dot{u}_0 = 0$ and $\ddot{u}_0 = -\omega_n^2 u_0$ (the initial condition for the acceleration was proposed by [19]). To put in evidence the effect of the parameters β and ζ, three different cases are studied:

- Case 1: The electrical parameters L and R take the value of the reference case of the validation of Section 4.2, $L_1 = L_0 = 7.83$ μH and $R_1 = R_0 = 5.97$ mΩ, *i.e.* the non-viscous damping factor and the viscous damping factor are also the same as the reference system, $\beta_1 = \beta_0 = 0.051$ and $\zeta_1 = \zeta_0 = 0.0055$.
- Case 2: Both the self-inductance and resistance parameters are reduced by 400 times, $L_2 = L_0/400 = 19.58$ nH and $R_2 = R_0/400 = 14.93$ $\mu\Omega$. Then, the non-viscous damping factor does not vary, $\beta_2 = \beta_0 = 0.051$, and the viscous damping factor is multiplied by 400, $\zeta_2 = 400\zeta_0 = 2.2$.
- Case 3: The resistance is the same as the Case 2, $R_3 = R_0/400 = 14.93$ $\mu\Omega$, but the self-inductance is reduced only 10 times, $L_3 = L_0/10 = 0.783$ μH. This implies that the viscous damping factor is the same as the Case 2, $\zeta_3 = 400\zeta_0 = 2.2$, but the non-viscous damping factor is multiplied by 40, $\beta_3 = 40\beta_0 = 2.04$.

The numerical values of these study cases are chosen to reveal different behaviour that the Zener model is able to reproduce and the viscous one is not. The response of the system is computed at the time corresponding 5 times the natural period of the system, $t_{max} = 5T_n = 5/f_n$. The normalised response $u(t)/u_0$ of the three study cases are represented in Fig. 7 as a function of the normalised time t/T_n.

To analyse these curves, it is important to take into account some properties of the Zener model that differentiate it from the Kelvin-Voigt model. The behaviour of the Kelvin-Voigt model may be underdamped, critically damped or overdamped depending of the value of the viscous damping factor ζ compared with the critical value that is equal to 1. However, the Zener model has two different critical damping factors, namely the critical viscous damping factor $\zeta_{cr} = 4/3\sqrt{3}$ and the critical non-viscous damping factor $\beta_{cr} = 1/3\sqrt{3}$. A deep study of the behaviour of the Zener model depending of the values of the damping factors is carried out by Adhikari in [21].

Next, the following conclusions are derived from Fig. 7:

- Case 1 presents a lightly damped vibratory behaviour, in which the normalised amplitude is reduced from 1 to 0.84 in 5 periods. This corresponds to an underdamped system, because the viscous damping factor is smaller than the critical value $\zeta < \zeta_{cr}$.
- On the contrary, Case 2 does not show vibration, *i.e.* it is an overdamped system. This is because the viscous damping factor is bigger than the critical value $\zeta > \zeta_{cr}$ and the non-viscous damping factor is smaller than the corresponding critical value $\beta < \beta_{cr}$.
- However, Case 3 corresponds to a particular case of the Zener model that can not be reproduced by the Kelvin-Voigt model. In Case 3, the system vibrates but the oscillatory behaviour does not cross the zero value, *i.e.*, the vibrations happen around a variable equilibrium position governed by the non-viscous mode (see *e.g.* Ref. [19] for details about the modes of the Zener model). This is because the viscous damping factor is bigger than the critical value $\zeta > \zeta_{cr}$ like in Case 2, but the non-viscous damping factor is bigger than the critical value $\beta > \beta_{cr}$.

Concluding, in this section it has been shown that the electrical properties of the system have influence on the mechanical behaviour of the system when it is subjected to a magnetic field and eddy currents appear. This influence can be studied by means of the equivalent viscoelastic Zener model trough the damping factors related with the electrical properties.

6. Conclusion

In this paper the eddy currents damping appearing in a metallic object moving in a uniform magnetic field has been explained as Zener viscoelastic damping, namely, the effect of the eddy currents damping is equivalent to that of viscoelasticity.

To find this equivalence, the eddy currents have been modelled by a coupled mechanical-electrical system for two different excitations, a harmonic force and a base motion. It has been found that the governing equations of the coupled system contains terms of derivatives of the displacement up to the third order, the same as in a viscoelastic system modelled with a Zener model. In viscoelasticity, the third order derivative term is related with relaxation, one of the main properties of viscoelasticity. It has been found that, in the case of the eddy currents damping, the relaxation is provided by the self-inductance of the object. The relaxation implies forces proportional to the jerk, which explains some experimental results [16]. In addition, the Zener model is a linear model that has been widely studied in the literature, as opposed to non-linear models proposed by other authors to explain similar properties as the forces proportional to the third derivative of the displacement [17,23]. These other non-linear models are based on the Kelvin-Voigt model in which the viscous damping coefficient c is not a constant and the system is no longer linear. However, by means of the Zener model, the well-known properties of the linear viscoelasticity can be directly extrapolated to the systems with eddy currents damping.

The validation of the analogy has been carried out in two different ways. On the one hand, an analytical validation that consists in the comparison of the forced response with a model of the literature. On the other hand, the validation comes from the experimental transmissibility data of an aluminium cantilever beam vibrating in a magnetic field.

A parametric study has been presented to reveal the influence that the magnetic field intensity and the electrical properties of the system has on its mechanical response. Specifically, it has been studied the influence of the magnetic field intensity on the frequency response and the influence of the electrical properties on the time response. In this manner, it has been revealed how the magnetic field intensity influences on the attenuation of the system. Also, it has been shown that the system has vibratory behaviour or not depending

on the magnitude of electrical properties of the system.

Concluding, this paper shows that for practical engineering applications as the design of eddy currents dampers, the utilisation of the properties of the well-known Zener model, could help designers to improve the effectiveness of their designs.

CRediT authorship contribution statement

Fernando Cortés: Conceptualization, Investigation, Methodology, Validation. **Ondiz Zarraga:** Software, Writing – original draft. **Imanol Sarría:** Investigation, Writing – review & editing. **María Jesús Elejabarrieta:** Visualization, Conceptualization, Supervision.

Declaration of Competing Interest

None.

Data availability

Data will be made available on request.

Acknowledgements

This study received financial support from the Department of Education of the Basque Government for the Research Group program IT1507–22.

References

[1] A.Alonso Rodríguez, E. Bertolazzi, R. Ghiloni, A. Valli, Finite element simulation of eddy current problems using magnetic scalar potentials, J. Comput. Phys. 294 (2015) 503–523, https://doi.org/10.1016/j.jcp.2015.03.060.
[2] G. Sinha, S.S. Prabhu, Force on a storage ring vacuum chamber after sudden turn-off of a magnet power supply, Phys. Rev. Spec. Top. - Accel. Beams. 14 (2011), 102401, https://doi.org/10.1103/PhysRevSTAB.14.102401.
[3] C.V. Dodd, W.E. Deeds, Analytical Solutions to Eddy-Current Probe-Coil Problems, J. Appl. Phys. 39 (1968) 2829–2838, https://doi.org/10.1063/1.1656680.
[4] E.C. Okress, D.M. Wroughton, G. Comenetz, P.H. Brace, J.C.R. Kelly, Electromagnetic Levitation of Solid and Molten Metals, J. Appl. Phys. 23 (1952) 545–552, https://doi.org/10.1063/1.1702249.
[5] E. Fromm, H. Jehn, Electromagnetic forces and power absorption in levitation melting, Br. J. Appl. Phys. 16 (1965) 653–663, https://doi.org/10.1088/0508-3443/16/5/308.
[6] M.A. Heald, Magnetic braking: Improved theory, Am. J. Phys. 56 (1988) 521–522, https://doi.org/10.1119/1.15570.
[7] J. Li, G. Yang, Equivalent subdomain method for performance prediction of permanent magnet eddy current brakes, IET Electr. Power Appl. 15 (2021) 1174–1186, https://doi.org/10.1049/elp2.12087.
[8] Z. Lu, B. Huang, Q. Zhang, X. Lu, Experimental and analytical study on vibration control effects of eddy-current tuned mass dampers under seismic excitations, J. Sound Vib. 421 (2018) 153–165, https://doi.org/10.1016/j.jsv.2017.10.035.
[9] B. Yan, Z. Wang, H. Ma, H. Bao, K. Wang, C. Wu, A novel lever-type vibration isolator with eddy current damping, J. Sound Vib. 494 (2021), 115862, https://doi.org/10.1016/j.jsv.2020.115862.
[10] H.A. Sodano, Eddy Current Damping in Structures, Shock Vib. Dig. 36 (2004) 469–478, https://doi.org/10.1177/0583102404048517.
[11] E. Diez-Jimenez, R. Rizzo, M.-J. Gómez-García, E. Corral-Abad, Review of Passive Electromagnetic Devices for Vibration Damping and Isolation, Shock Vib. 2019 (2019) 1–16, https://doi.org/10.1155/2019/1250707.
[12] H.A. Sodano, J.-S. Bae, D.J. Inman, W.Keith Belvin, Concept and model of eddy current damper for vibration suppression of a beam, J. Sound Vib. 288 (2005) 1177–1196, https://doi.org/10.1016/j.jsv.2005.01.016.
[13] H.A. Sodano, J.-S. Bae, D.J. Inman, W.K. Belvin, Improved Concept and Model of Eddy Current Damper, J. Vib. Acoust. 128 (2006) 294–302, https://doi.org/10.1115/1.2172256.
[14] Turner, L.R., & Hua, T.Q., Experimental study of coupling between eddy currents and deflections in cantilevered beams as models of tokamak limiters (CONF-8610240–1). United States (1986).
[15] James R. Nagel, Fast Finite-Difference Calculation of Eddy Currents in Thin Metal Sheets, Appl. Comput. Electromagn. Soc. J. 33 (2018) 575–584.
[16] C.N. Loong, J. Shan, Z. Shi, C.-.C. Chang, Approximate analysis of eddy-current force under time-varying velocity motion for structural control, J. Sound Vib. 475 (2020), 115295, https://doi.org/10.1016/j.jsv.2020.115295.
[17] Z. Shi, C.N. Loong, J. Shan, Equivalent circuit model of eddy current damping regarding frequency-dependence with test validation, Adv. Struct. Eng. 25 (2022) 188–200, https://doi.org/10.1177/13694332211050989.
[18] L. Irazu, M.J. Elejabarrieta, Magneto-dynamic analysis of sandwiches composed of a thin viscoelastic-magnetorheological layer, J. Intell. Mater. Syst. Struct. 28 (2017) 3106–3114, https://doi.org/10.1177/1045389X17705209.
[19] J. García-Barruetabeña, F. Cortés, J.M. Abete, Dynamics of an exponentially damped solid rod: Analytic solution and finite element formulations, Int. J. Solids Struct. 49 (2012) 590–598, https://doi.org/10.1016/j.ijsolstr.2011.11.004.
[20] B.M. Notaros, Electromagnetics, Prentice Hall, Upper Saddle River, 2011.
[21] S. Adhikari, Qualitative dynamic characteristics of a non-viscously damped oscillator, Proc. R. Soc. Math. Phys. Eng. Sci. 461 (2005) 2269–2288, https://doi.org/10.1098/rspa.2005.1485.
[22] R.D. Blevins, Formulas For Natural Frequency and Mode Shape, Krieger Publishing, Malabar, Florida, 2001. Reprint ed.
[23] Z. Shi, J. Shan, C.N. Loong, W. Wu, C.-.C. Chang, W. Shi, Experimental and Numerical Study on Dynamic Behavior of Eddy Current Damping with Frequency Dependence, J. Eng. Mech. 146 (2020), 04020116, https://doi.org/10.1061/(ASCE)EM.1943-7889.0001852.